

Review

Anthracene-Containing Metallacycles and Metallacages: Structures, Properties, and Applications

Jian-Hong Tang^{1,*} and Yu-Wu Zhong^{1,2,*} 

¹ Beijing National Laboratory for Molecular Sciences, CAS Key Laboratory of Photochemistry, CAS Research/Education Center for Excellence in Molecular Sciences, Institute of Chemistry, Chinese Academy of Sciences, Beijing 100190, China

² School of Chemical Sciences, University of Chinese Academy of Sciences, Beijing 100049, China

* Correspondence: tangjianhong@iccas.ac.cn (J.-H.T.); zhongyuwu@iccas.ac.cn (Y.-W.Z.); Tel.: +86-010-62652950 (Y.-W.Z.)

Abstract: Due to its highly conjugated panel-like structure and unique photophysical and chemical features, anthracene has been widely used for fabricating attractive and functional supramolecular assemblies, including two-dimensional metallacycles and three-dimensional metallacages. The embedded anthracenes in these assemblies often show synergistic effects on enhancing the desired supramolecular and luminescent properties. This review focuses on the metallasupramolecular architectures with anthracene-containing building blocks, as well as their applications in host-guest chemistry, stimulus response, molecular sensing, light harvesting, and biomedical science.

Keywords: anthracene; metallacycles; metallacages; host-guest chemistry; stimulus response; molecular sensing; light harvesting; biomedical science



Citation: Tang, J.-H.; Zhong, Y.-W. Anthracene-Containing Metallacycles and Metallacages: Structures, Properties, and Applications. *Inorganics* **2022**, *10*, 88. <https://doi.org/10.3390/inorganics10070088>

Academic Editors: Rainer Winter and Bruno Therrien

Received: 6 June 2022

Accepted: 20 June 2022

Published: 22 June 2022

Publisher's Note: MDPI stays neutral with regard to jurisdictional claims in published maps and institutional affiliations.



Copyright: © 2022 by the authors. Licensee MDPI, Basel, Switzerland. This article is an open access article distributed under the terms and conditions of the Creative Commons Attribution (CC BY) license (<https://creativecommons.org/licenses/by/4.0/>).

1. Introduction

The construction of discrete supramolecular metallacycles and metallacages with well-defined sizes, shapes, and geometries has attracted considerable attention [1–6]. Based on the coordination-driven self-assembly strategy, the spontaneous formation of metal-ligand coordination bonds between Lewis-basic organic donor and Lewis-acidic metal acceptor fabricates a large number of two-dimensional (2D) and three-dimensional (3D) metallasupramolecular architectures, such as molecular triangles, squares, hexagons, polygons, polyhedrons, etc., [7–11]. The high directionality and relative strong strength of coordination bonds offer the possibility of introducing multiple functional units into metallasupramolecular structures with precise stoichiometric and spatial arrangement of individual moieties [12,13]. The incorporation of functional building blocks with favorable photophysical/chemical properties into these metallasupramolecular structures remains an effective means to pursue desired behavior and applications.

Among various functional blocks, anthracene derivatives have been extensively utilized in the fabrication of supramolecular coordination assemblies [14,15]. The large conjugated π -system and panel-like structure of anthracene endow robust photophysical and photochemical behavior, such as rich absorption and emission spectra, high fluorescence quantum yields, and ordered aromatic-aromatic interactions [16,17]. In order to incorporate anthracene into metallasupramolecular structures, the chemical modification of the anthracene core is usually required. In general, in line with the coordination-driven self-assembly methodology, the incorporation of anthracene moieties into metallasupramolecular structures can be achieved with either an anthracene-containing ligand as a Lewis-basic organic donor or a transition-metal moiety as a Lewis-acidic metal acceptor. It represents a facile way to develop anthracene-based organic donors by integrating anthracene with diverse organic ligands such as pyridyl [18], pyrazolyl [14,19], imidazolyl [20], or *N*-heterocyclic carbene (NHC) ligand [21]. The functionalized organic donors can subsequently react with

metal salts or organometallic motifs to afford target metallasupramolecules. In addition, some efforts have been devoted to preparing the anthracene-functionalized transition metal acceptors, which are capable of directly reacting with corresponding organic ligands to form coordination assemblies [22,23]. The anthracene-incorporated metallasupramolecular structures are featured by tunable cavity enclosure, favorable aromatic interactions, and appealing photoluminescent properties, resulting in a wide range of potential applications in host-guest chemistry, stimulus response, molecular sensing, light harvesting, and biomedical aspects [14,24–34].

In this review, we focus on the recent advance of the structural modifications, properties, and potential applications of anthracene-containing metallacycles and metallacages. Specifically, the anthracene-functionalization strategies for constructing metallasupramolecules and the representative advance in exploring the properties and applications of these metallasupramolecules are discussed.

2. Constructions of Anthracene-Containing Metallacycles and Metallacages

In order to construct discrete supramolecular metallacycles and metallacages via the coordination-driven self-assembly, the introduction of the direction-controlled metal–ligand interactions between complementary precursors is necessary. The precursors with pre-defined angles and symmetries react in a specific ratio to produce the well-defined supramolecular assemblies. The anthracene group can be incorporated into metallacycles and metallacages by using either the anthracene-containing organic donor or organometallic acceptor building blocks.

2.1. Anthracene-Containing Organic Donor Building Blocks

The combination of the anthracene moiety with organic coordination groups affords the rigid and versatile functional building blocks. After reacting with the complementary metallic reagents, a number of anthracene-based coordination assemblies have been documented including metallacycles and metallacages. In general, the nitrogen-based coordination linkers have been mostly employed in constructing discrete supramolecular structures compared to the metal–carbon or metal–oxygen coordination-driven self-assembly. For instance, ligand 1,8-bis(4-pyridylethynyl)anthracene (**1**) has been used as a rigid nitrogen-based organic “clip” to construct both rectangles and trigonal prisms (Figure 1). Considering the flexible coordination sphere of the 3d-metal ions, the equimolar reactions of **1** with 3d-metal acetate linear linkers such as Mn(II), Zn(II), or Cu(II) acetates result in the formation of either rectangular (**2**) or zigzag polymeric (**3**) structures [35]. However, after changing the metal linkers to 1,4-bis[*trans*-Pd(PEt₃)₂(NO₃)(ethynyl)]benzene (**7**), it only affords the rectangle product **4** due to the rigid square planar coordination environment of Pd(II) [36,37]. The similar phenomenon was also observed for the other square planar coordination metal linkers such as Pt(II) complexes [38,39]. The half-sandwiched Ru^{II}₂ metal precursor [Ru₂(μ-η⁴-C₂O₄)(MeOH)₂(η⁶-p-cymene)₂](O₃SCF₃)₂ (**8**) has also been demonstrated to react with **1** in 1:1 molar ratio to form the 2D metallacycle **5** [40]. Moreover, the 3D nanoscopic prismatic cage **6** with tunable shape, size, and properties was fabricated by mixing the tritopic Pt(II) linker 1,1,1-tris[4-(*trans*-Pt(PEt₃)₂(NO₃))phenyl]ethane (**9**) with **1** in 2:3 molar ratio [41,42]. Recently, Jin, Hahn, and co-workers presented a series of iridium(III) metalla[2]catenanes prepared from a non-linear but rigid dipyriddy donor ligand 1,5-bis(4-pyridylethynyl)anthracene [43]. Due to the nonlinear structure and aromatic π–π and C–H⋯π interactions of the ligand, the controlled transformations between tetranuclear metallarectangles and metalla[2]catenanes were realized in solution by changing the solvent, concentration, or guest species. In addition, the incorporation of halogen atoms into the dinuclear metal complex bridge led to interlocked metalla[2]catenanes with two different topological configurations in the solid state.

Besides the nitrogen-based organic donor ligands, the strong σ-donating NHC can form stable metal–carbon bonds to generate supramolecular structures. The NHC coordination complexes exhibit unusual chemical-physical properties and show promising

applications in catalysis [44–46], sensing [47], and medicine chemistry [48]. Zhang and co-workers integrated NHCs with supramolecular host calixarene fragments to synthesize the dinuclear Ag(I) metallamacrocycles functionalized with multi-anthracene groups [49]. As shown in Figure 2a, the anthracene-capped NHC ligand precursor **10** reacted with Ag₂O to afford metallacycle **11**. X-ray diffraction analysis indicated that 2D supramolecular layer (Figure 2b) and 3D supramolecular network (Figure 2c) were observed by viewing along the different axis of **11**. The 3D network was assembled by the π – π interactions of the intermolecular anthracene rings with a face-to-face separation of 3.367 Å and the C–H...F interactions among PF₆[−] anions and various proton atoms. The configurations of the metallacycle structures can also be modulated by changing the upper-rims of calixarenes or the *N*-substituents of the carbene ligand [49].

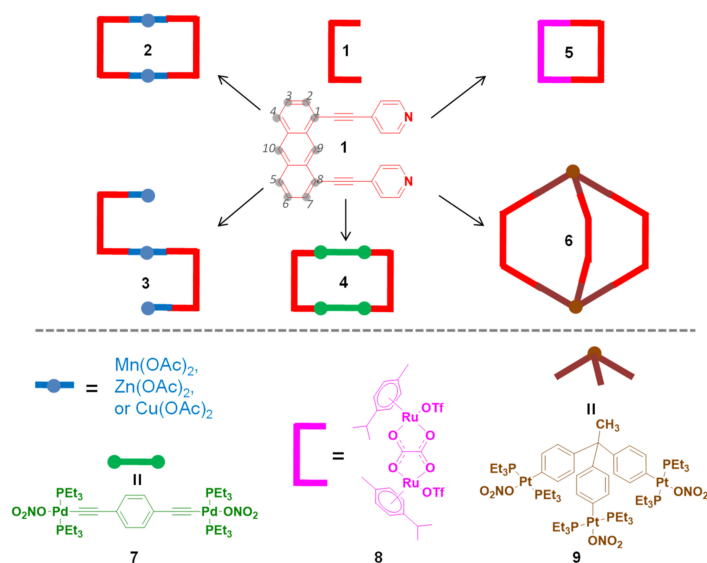


Figure 1. Nitrogen-based anthracene-containing ligand **1** for constructing coordination self-assemblies. The numbering scheme for the carbon atoms in anthracene is displayed along with the structure of ligand **1**.

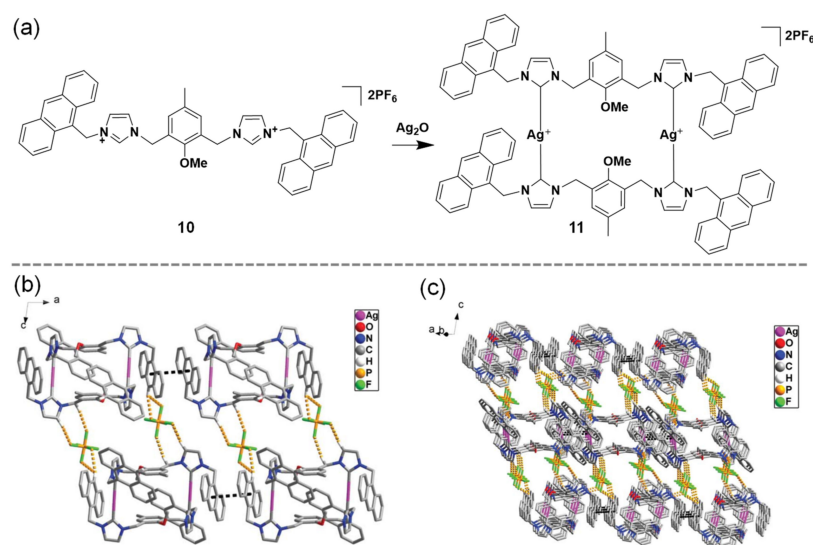


Figure 2. *N*-heterocyclic carbene-based anthracene-containing ligand precursor **10** for constructing coordination self-assemblies. (a) Synthesis of metallacycle **11**. (b) The 2D supramolecular layer of **11** viewed along the *b* axis. (c) The 3D supramolecular network of **11** viewed along the *a* axis. Reprinted with permission from Ref. [49]. Copyright 2013 Royal Society of Chemistry.

2.2. Anthracene-Containing Organometallic Acceptor Building Blocks

As an alternative approach to the organic donor linkers, anthracene has also been modified as the organometallic acceptor building blocks to construct coordination assemblies. The combination of metals with organic ligands usually simplifies the multi-component self-assembly. A handful of research interests have been focused on the 1,8-metallated anthracene congeners due to their parallel coordination environment [50–52]. By using bridging linkers with nitrogen- to oxygen-based organic coordination ligands, both supramolecular rectangles and cages have been developed via two-component self-assembly as discussed below.

Based on the dipyriddy-based coordination linkers, as shown in Figure 3, the Stang group fabricated the first series of 2D molecular rectangles via the assembly of a 1,8-diplatinum(II)-functionalized anthracene organometallic “clip” (**12**) with the linear ligand **15** or **16** [22]. Scanning tunneling microscopy investigations indicated that the long edge of the rectangle **13** stood on the surface and exhibited a 2D molecular network on pyrolytic graphite, while the rectangle face of **13** laid flat on the Au(111) surface showing linear chains [53]. The same group also reported a family of the propeller-type 3D supramolecular cages **14** with dimensions of 1×2 nm to 1×4 nm by the use of the tritopic pyridyl subunit **17** or **18** [54]. The size- and shape-selective self-sorting process in both 2D rectangles and 3D cages was also unveiled [55,56]. Mukherjee and co-workers extended the above methodology by incorporating the ethynyl unit into a new anthracene-containing organometallic Pt^{II}_2 “clip” molecule. They further introduced the four-imine-containing dipyriddy blocks to synthesize molecular rectangles, which showed reversible fluorescent responses to $\text{Fe}^{3+}/\text{Cu}^{2+}/\text{Ni}^{2+}$ via the metal coordination-triggered photo-induced electron transfer mechanism [34].

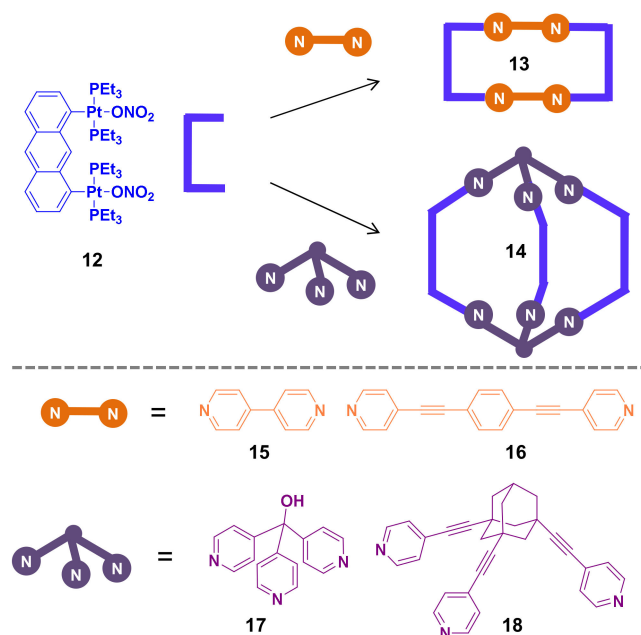


Figure 3. Diplatinum(II)-based anthracene-containing linker **12** for constructing nitrogen-based 2D and 3D coordination self-assemblies.

Anionic oxygen donors represent another type of simple coordination building blocks, which have been widely used to prepare supramolecular structures. As shown in Figure 4a, the 1:1 stoichiometric reactions of the 1,8-diplatinum(II) “clip” **12** with the linear dicarboxylate-based oxygen linker **19** or **20** produced the corresponding rectangles **21** and **22**. Single crystal X-ray analysis of the obtained assemblies confirmed the formation of the Pt–O bonds (Figure 4b) [57]. Inspired by this pioneering work, a number of functionality-directed metal–oxygen–bond-containing macrocycles were reported by incorporating various functional groups into the dicarboxylate linkers such as ferrocene [58], carborane [59], crown ether [60], and chiral species [61]. The modulation of the organometallic Pt^{II} “clip” to Pd^{II} architectures

has also been demonstrated by forming Pd–O bonds [62,63]. Moreover, Pluth and co-workers described an asymmetrical pyridyl quinolone ligand that was able to form hybrid metal–oxygen and metal–nitrogen bonds in the self-assembled macrocycle, which further expanded the library of metal–ligand-derived supramolecular architectures [64].

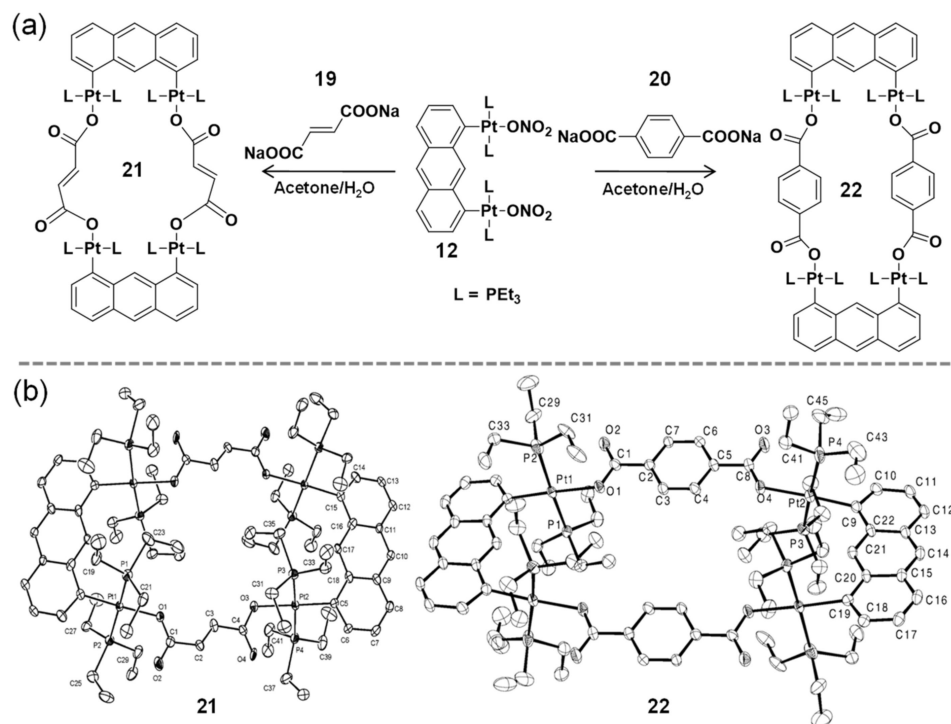


Figure 4. Diplatinum(II)-based anthracene-containing linker 12 for constructing oxygen-based rectangles. (a) The formation of molecular rectangles 21 and 22. (b) ORTEP diagrams of 21 and 22. Reprinted with permission from Ref. [57]. Copyright 2003 American Chemical Society.

3. Properties and Applications of Anthracene-Containing Metallacycles and Metallacages

The anthracene-containing metallacycles and metallacages combine multi-functional units into the well-defined discrete supramolecular architectures with extended π -surfaces and modifiable cavities and shapes. The resulting assemblies not only display the diversity of structural aspects, but also endow a wide range of intriguing properties and applications. In this section, we discuss the representative properties and potential applications of some recently developed anthracene-based supramolecules in the fields of host-guest chemistry, stimulus response, molecular sensing, light harvesting energy transfer, and biomedical science.

3.1. Host-Guest Chemistry

Host-guest chemistry represents one of the most important features of supramolecular assemblies. The construction of unique host-guest structures initiates numerous fundamental investigations and applied explorations in the fields of fluorescence, catalysis, drug delivery, etc., [65–69]. Among various supramolecular hosts, anthracene-containing 2D metallacycles and 3D metallacages have been well-explored because of their rigid aromatic surfaces and unique photophysical and photochemical properties.

As shown in Figure 5, Chi and co-workers disclosed the reversible structural transformations between monorectangle and metalla[2]catenane via guest- and solvent-dependent self-assembly [70]. The assembly of the tetracene-based diruthenium(II) acceptor 23 and the anthracene-functionalized dipyridyl donor 24 afforded multiple stimulus-responsive supramolecular structures. Specifically, the [M₂L₂] monorectangle structure 25 was obtained in an equivalent molar mixing of the donor and acceptor linkers in nitromethane (CH₃NO₂). After changing the solvent to methanol (CH₃OH), an interlocked [M₂L₂]₂

metalla[2]catenane **26** with strong π - π interactions was formed. Interestingly, the addition of pyrene into the identical reaction in methanol generated the pyrene-encapsulated host-guest complex $[(\text{pyrene})_2\subset\mathbf{25}]$. X-ray crystal structure studies indicated that two pyrene guests were bound in the aromatic cavity of **25** via host-guest interactions.

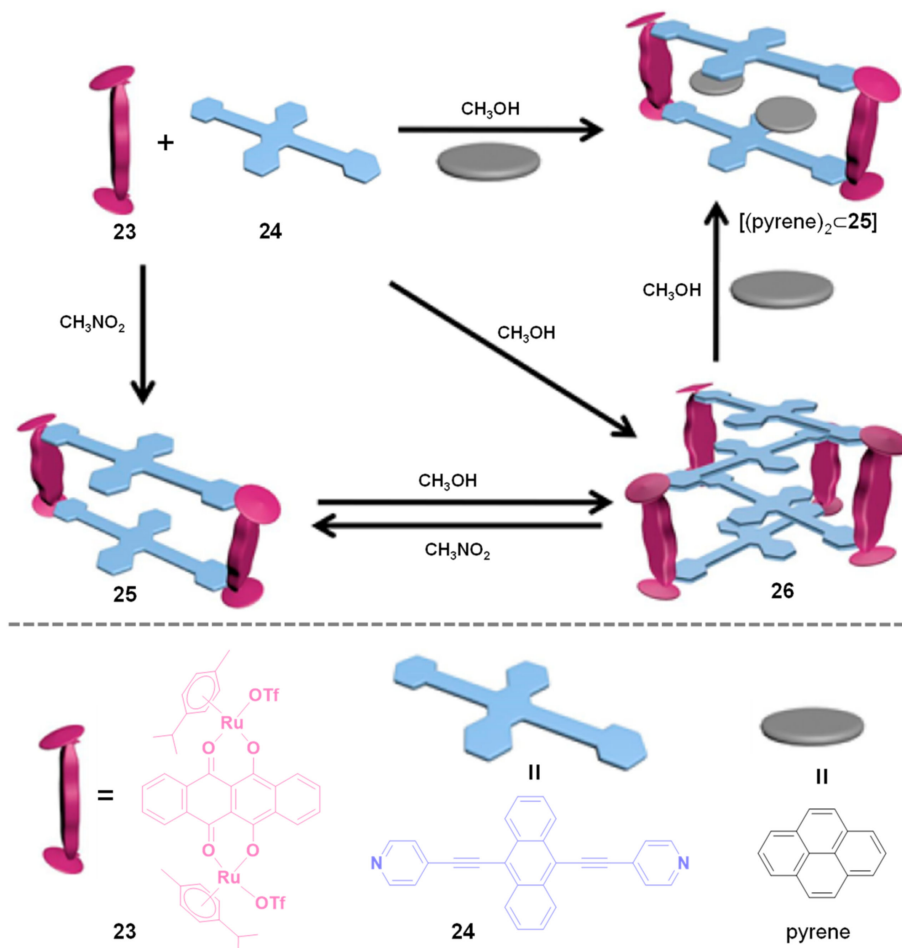


Figure 5. The reversibly fine-tuned self-assembly among monorectangle and catenane structures. Reprinted with permission from Ref. [70]. Copyright 2015 American Chemical Society.

Compared to metallacycle-based hosts, metallacages or capsules can introduce more tight and selective binding affinity for large guest substrates. For example, the Nitschke group employed a C_2 -symmetric 1,5-diaminoanthracene **27** building block to generate the anthracene-edged $\text{Fe}^{\text{II}}_4\text{L}_6$ tetrahedral cage **28** (Figure 6a) [24]. The Diels-Alder cycloadditions of the six anthracene panels of **28** with the electron-deficient dienophile reagent such as tetracyanoethylene (TCNE) yielded the new cage **29**. The modified cage **29** possessed an enclosed cavity suitable for the encapsulation of the fullerene C_{60} to give the host-guest complex $[\text{C}_{60}\subset\mathbf{29}]$. In contrast, the treatment of the original cage **28** with C_{60} formed a covalent adduct $[\text{C}_{60}\cdot\mathbf{28}]$ through the Diels-Alder cycloadditions of three of its anthracene ligands with C_{60} . The remaining three anthracene ligands of $[\text{C}_{60}\cdot\mathbf{28}]$ can further react with TCNE to give a new product (structure not shown) by post-assembly modification. These topologically controlled modifications would be unable to access if the reaction components were added together before assembly. As shown in Figure 6b, X-ray diffraction analysis of $[\text{C}_{60}\cdot\mathbf{28}]$ and $[\text{C}_{60}\subset\mathbf{29}]$ confirmed the tetrahedral cage structure and the covalent Diels-Alder cycloaddition reactions of TCNE and C_{60} with the iron cage.

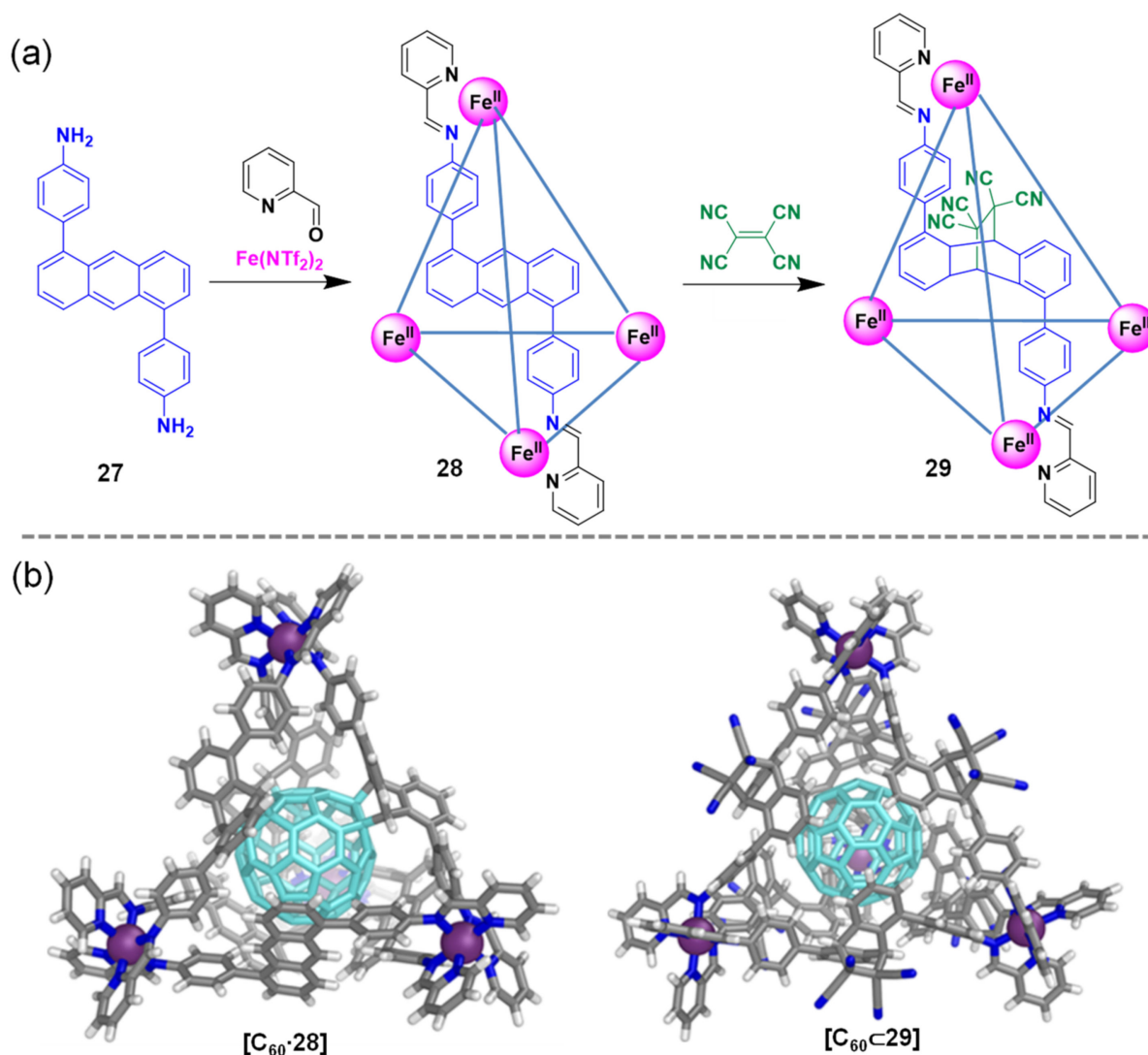


Figure 6. Anthracene-edged iron cages. (a) Formation of cage 28 and its post-modification with tetracyanoethylene to give 29. (b) The crystal structures of the covalent adduct $[\text{C}_{60}\cdot 28]$ and the host-guest complex $[\text{C}_{60}\subset 29]$. Reprinted with permission from Ref. [24]. Copyright 2016 American Chemical Society.

Yoshizawa and co-workers designed a new bent bispyridine-anthracene linker 30 with an orthogonal conformation of the aromatic sub-units [30]. The combination of $\text{Pd}(\text{II})$ ions and 30 in a 1:2 molar ratio afforded the formation of a M_2L_4 capsule 31 possessing a cavity with a diameter around 1 nm (Figure 7a). The encapsulations of the medium-sized spherical guest [2,2]paracyclophane 32 and the planar guest 1-methylpyrene 33 were monitored by ^1H NMR techniques (Figure 7b–d). The X-ray crystal structure of the host-guest scaffold $[(33)_2\subset 31]$ further demonstrated that the cavity of 31 was able to encapsulate two guest molecules of 33. Moreover, the larger molecule fullerene (C_{60}) also formed host-guest complexes with 31 in quantitative yields. The same group expanded the above platform to $\text{Pt}(\text{II})$ -linked coordination capsules using the same bispyridine-anthracene skeleton with different metal ions and substitutes [71]. The highly emissive host-guest complexes with fluorescence quantum yields up to 0.5 were successfully obtained by the encapsulation of various molecular dyes such as 4,4'-difluoro-4-bora-3a,4a-diaza-s-indacene (BODIPY) and coumarin derivatives.

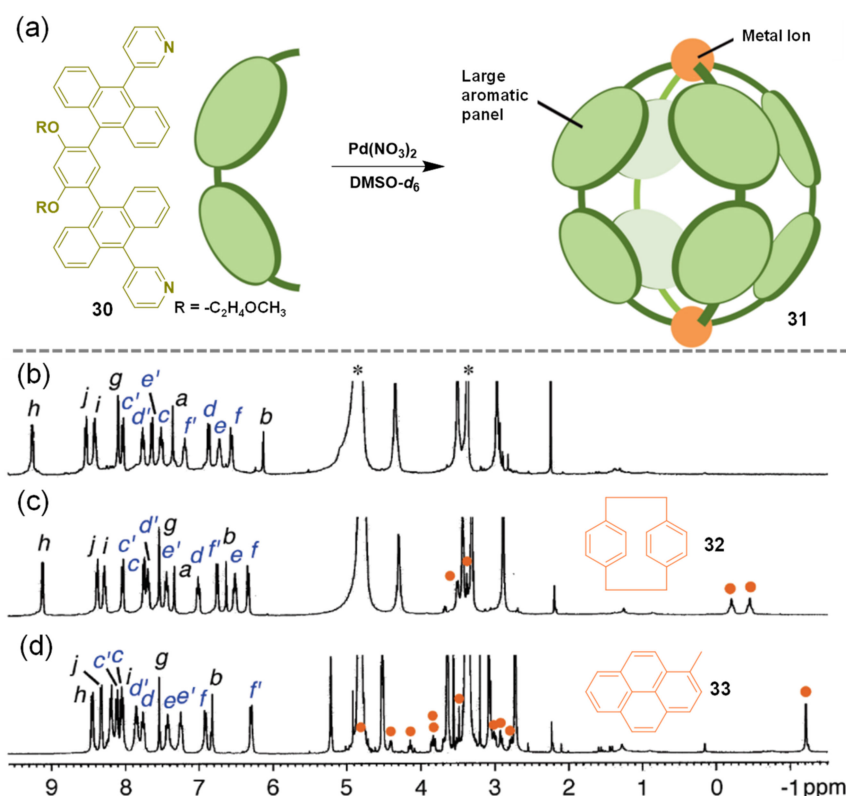


Figure 7. Self-assembly and host-guest chemistry of molecular capsule 31. (a) Schematic representation of the formation of 31. (b–d) ¹H NMR spectra of (b) 31, (c) [32C31], and (d) [(33)₂C31]. Orange signals are from the encapsulated guest 32 or 33. *: solvent signals. Reprinted with permission from Ref. [30]. Copyright 2011 American Chemical Society.

3.2. Stimulus Response

Stimulus response can be defined as the phenomenon that the substrates are capable of altering their structural and/or physical–chemical properties in response to external stimulus such as temperature, light irradiation, pressure, chemicals, solvent, and so on. The development of stimulus-responsive materials has attracted extensive research interests in order to mimic bioprocesses and explore functional materials [72–75]. Anthracene-based supramolecular architectures with intriguing photophysical, photochemical, and host-guest behavior represent a promising category of stimulus-responsive material candidates. For instance, three or six freely rotating anthracene groups have been incorporated into organoplatinum(II) hexagonal metallacycles to show temperature-responsive behavior (Figure 8). The treatment of the 120° anthracene-functionalized triarylamine ligand 34 with the 120° diplatinum(II) acceptor 35 or the 180° diplatinum(II) acceptor 36 generated the [3 + 3] or [6 + 6] hexagonal metallacycles 37 and 38, respectively [76]. The resulting assemblies exhibited reversible fluorescent response in tetrahydrofuran (THF) upon temperature variation from −20 to 60 °C (Figure 8b). However, in coordinating solvent such as dimethyl formaldehyde (DMF), they showed two-stage responses (Figure 8c). In the lower temperature range (below 30 °C), the emission spectral changes were similar to those observed in THF. At higher temperatures, the metallacycles were destroyed by the solvents and exhibited ratiometric fluorescent response. The further development of a dianthracene-based rhomboidal organoplatinum(II) metallacycle showed both temperature and mechanical-force dependent fluorescence [77]. Very recently, Wang, Xu and co-workers studied the luminescence properties of the platinum(II) metallacycles with inner- and outer-modified 9,10-distyrylanthracene units, indicating that the modified position of fluorophores played a vital role in modulating the properties of supramolecular assemblies [78].

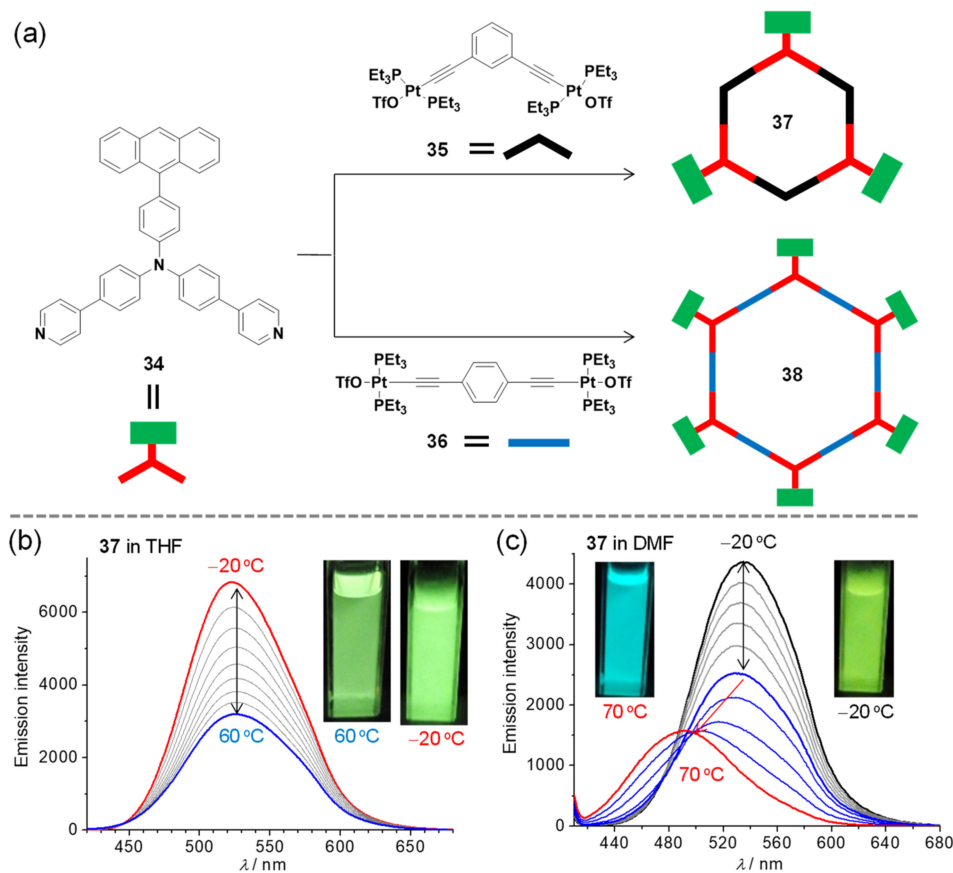


Figure 8. Temperature-responsive fluorescent metallacycles **37** and **38**. (a) Scheme of the syntheses of **37** and **38**. (b,c) Emission spectral changes of **37** in (b) THF and (c) DMF, respectively. The inset images show the solution under UV irradiation at specific temperature indicated. Reprinted with permission from Ref. [76]. Copyright 2018 American Chemical Society.

Photo-driving chemical transformations have been widely investigated in modern organic synthesis and materials science [79,80]. Anthracene-based derivatives usually show interesting photochemical reactions of anthracene at 9,10 positions, including [4 + 4] photodimerization and [4 + 2] oxygenation [81]. The integration of anthracene units into supramolecular architectures provides a versatile platform to achieve chemo- and region-selective photochemical transformations. The Han group reported the rhodium-based photoactive metallarectangle **39** containing the 2,6-di(1*H*-imidazol-1-yl) anthracene linker (Figure 9). The photochemical [4 + 4] cycloaddition of **39** regioselectively occurred to afford the *syn*-dimeric photo-addition product **40** in quantitative yield under irradiation at 365 nm, which could be clearly discerned from the ¹H NMR spectral changes [82]. The reversible transformation was further observed by thermal- or photo-induced (254 nm) cleavage reaction. Moreover, the pure organic photodimer **41** could be readily released from the metallarectangle in high yield (Figure 9d), which was difficult to access via conventional organic ligand-based reactions. Another rhodium-rectangle with a 2,7-bis(4-pyridyl)anthracene linker showed similar photo- and thermal response. The same group also employed the supramolecular templating strategy to other kinds of metallasupramolecular assemblies. For example, *N*-heterocyclic carbene- or azole-2,6-disubstituted anthracenes have been used to react with Ag(I) or Au(I) metallic reagents to generate metallacycles, which showed appealing regio- and stereo-selectivity on the photochemical [4 + 4] cyclodimerization [83].

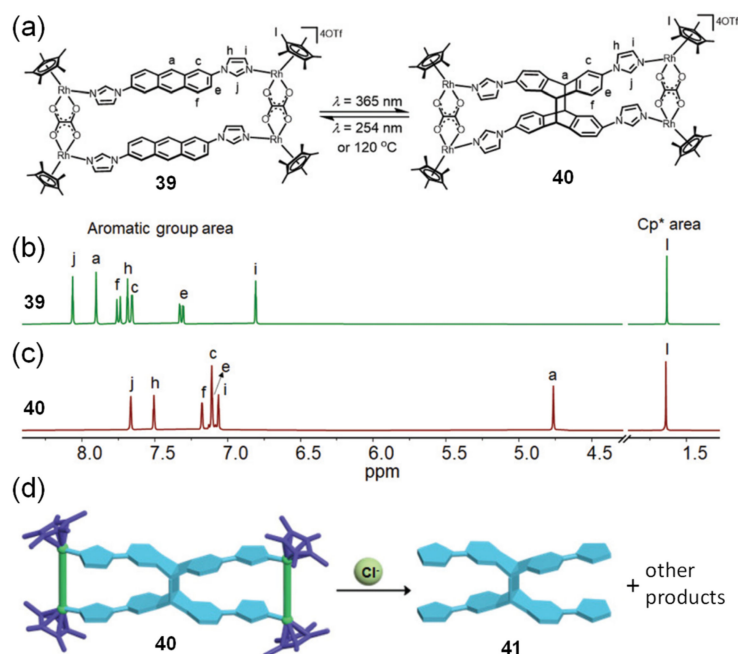


Figure 9. Stimulus-responsive rhodium-based metallarectangles. (a) Photochemical [4 + 4] cycloaddition of **39** and reversible transformation. (b,c) Partial ^1H NMR spectra in CD_3CN of (b) **39** and (c) **40**. (d) Schematic representation of the dissociation of **40** into **41**. Reprinted with permission from Ref. [82]. Copyright 2022 Royal Society of Chemistry.

The photochemical [4 + 2] oxygenation of anthracene-based supramolecular assemblies has also been demonstrated. Shionoya and co-workers reported the photosensitized oxygenation reactions in both liquid and solid conditions of a metallacycle containing multiple anthracene structures. As a result, the phase-dependent reactivity and host-guest interactions have been disclosed. Specifically, the photosensitized oxygenation reaction of metallacycle resulted in the fully oxygenated product in solution, whereas a mono-oxygenated C_s -symmetrical complex was provided in an amorphous solid state [84]. Our group introduced the reaction of a linear 9,10-bis(4-pyridyl)anthracene donor with a $\sim 120^\circ$ Pt(II) complementary acceptor to prepare a hexagonal metallacycle via the [6 + 6] coordination-driven self-assembly. The reversible capture and release of singlet oxygen in the resulting metallacycle were realized via combining photooxygenation with thermolysis processes [85].

3.3. Molecular Sensing

Molecular sensing can be generally considered as a sensor that interacts with an analyte to generate a detectable signal variation. The sensor molecule usually consists of two (or more) subcomponents that perform the recognition and signaling function, respectively. Selective and precise detection of target analytes is indispensable in a wide range of chemical, material, biological, environmental, and medical sciences [86–88]. Among these efforts, anthracene-containing metalla-supramolecular systems can incorporate multiple functional components into well-defined structures, providing the appropriate structural and chemical features for molecular sensing. Stang and co-workers developed a series of platinum(II)-based metallacycles for the selective and sensitive fluorescent detection of chemicals such as ammonia, nitroaromatics, amino acids, and so on [89,90]. As shown in Figure 10a, they employed the 9,10-di(4-pyridylvinyl)anthracene ligand (**42**) to react with dicarboxylates (**20** or **43**) and *cis*-(PEt_3) $_2$ Pt(OTf) $_2$ linkers for fabricating two near-infrared (NIR) emissive platinum(II) metallacycles **44** and **45** [91]. The resulting assemblies not only showed aggregation-induced emission (AIE) and solvatochromism behavior, but also exhibited NIR fluorescent detection of ammonia gas in the solid state (Figure 10b). The reversible

forming and breaking of the Pt-N coordination bonds was proposed for the observed emissive sensing properties. In addition, Mukherjee and co-workers synthesized a ditopic 180° Pt-ethynyl-based acceptor, which could react with the 1,8-bis(4-pyridylethynyl)anthracene (**1**) organic donor to yield an emissive metallamacrocycle [38]. The emission intensity of the metallamacrocycle was selectively and efficiently quenched in solution by the addition of picric acid, which is a common component in many chemical explosives. The charge-transfer processes between the electron-rich Pt-ethynyl-anthracene backbones and the electron-deficient nitroaromatic molecules were believed to be responsible for the resulting fluorescence quenching behavior.

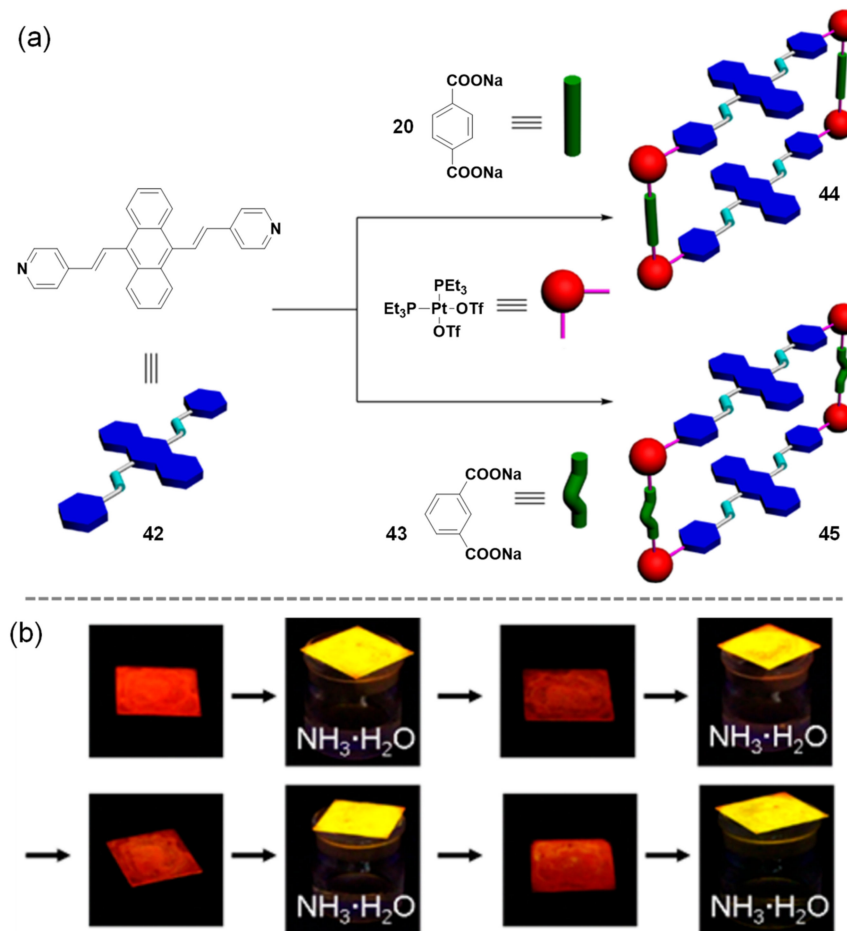


Figure 10. Near-infrared emissive discrete platinum(II) metallamacrocycles. (a) Synthesis of metallamacrocycles. (b) Photographs of films of **44** when exposed to or removed from ammonia under a UV lamp at 365 nm. Reprinted with permission from Ref. [91]. Copyright 2017 American Chemical Society.

Since 2008, the Yoshizawa group has continually worked on the bent anthracene dimer-based supramolecular capsules via the coordination-driven self-assembly approach to form M_2L_4 -type structures [15]. One of these examples, capsule **31**, has been discussed in Figure 7 [30]. The multiple anthracene panels of these capsules lead to a rigid spherical polyaromatic cavity. Various synthetic molecules and biomolecules have been successfully encapsulated in the cavity of the capsules through host-guest interactions. In particular, they have achieved the selective recognition of D-sucrose from natural saccharide mixtures in water with 100% selectivity and >85% yield using a Pt(II)-based multi-anthracene capsule [92]. The theoretical calculations and control experiments demonstrated that the multiple CH- π interactions and complementary shapes between the capsule and guest molecules contributed to the unique recognition properties.

3.4. Light Harvesting and Biomedical Applications

Due to the well-resolved absorption and strong emission properties of anthracene fluorophores, anthracene-based metallacycles and metallacages have ensured promising photo-active applications including light harvesting energy transfer and biomedical science [93,94]. Yang, Xu, and co-workers incorporated multiple anthracene, coumarin, and BODIPY fluorophores into a discrete hexagonal metallacycle with precise distances and locations based on the coordination-driven self-assembly and host–guest interactions [95]. The prepared assembly showed two-step fluorescence-resonance energy transfer (FRET) behavior, which resulted in a higher photosensitization efficiency of generating singlet oxygen and an enhanced photooxidation activity of a sulfide substrate compared to the corresponding one-step FRET system.

Very recently, Li and co-workers fabricated two trigonal prismatic metallacages **48** and **49** via a three-component self-assembly of two molecules of the trianthracene–triphenylamine-based tripyridyl ligand **46**, three molecules of dicarboxylate **20** or **47**, and six molecules of the 90° Pt(II) linker *cis*-(PEt₃)₂Pt(OTf)₂ (Figure 11a) [96]. Being beneficial from the well-organized multi-anthracene–triphenylamine moieties, the obtained cages displayed unique absorption and emission properties with high emission quantum yield and stimulus-responsive fluorescence (solvent polarity, temperature, and concentration). Moreover, the efficient FRET between the cage energy donor and the Nile Red (NR) energy acceptor was realized with an energy transfer efficiency of >93% at an acceptor/donor ratio of 15/1 (Figure 11b,c). The apparent static quenching mechanism was proposed for the efficient energy transfer process.

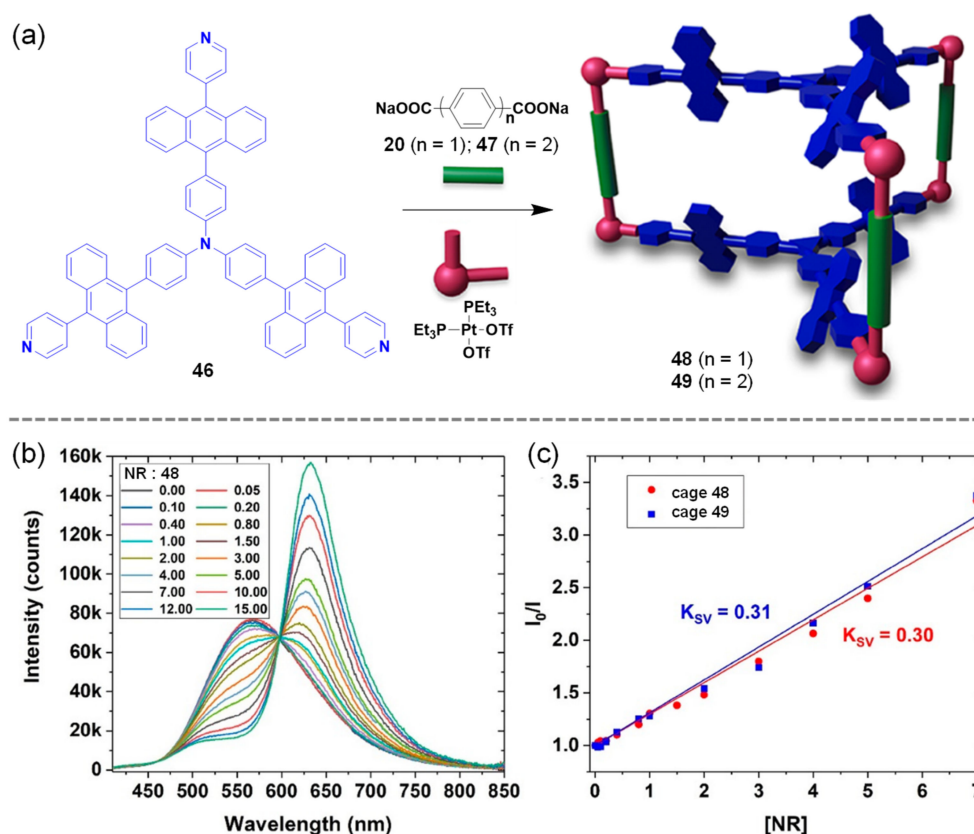


Figure 11. Trianthracene–triphenylamine-based platinum(II) metallacages **48** and **49** for light harvesting energy transfer. (a) Schematic representation of the syntheses of metallacages. (b) Emissive titration of **48** with varying amounts of Nile Red (NR). (c) The corresponding Stern–Volmer analyses of **48** and **49** in the presence of different concentration ratios of NR. Reprinted with permission from Ref. [96]. Copyright 2021 American Chemical Society.

Huang et al., reported a dual-emissive Pt(II) metallacage for *in vivo* hypoxia imaging and imaging-guided chemotherapy (Figure 12) [97]. In the molecular design, Pt(II)-meso-tetra(4-carboxyphenyl)porphine (**50**) was employed as an oxygen concentration responsive red phosphorescence unit, while the anthracene-based ligand **51** was selected as a blue fluorophore and *cis*-(PEt₃)₂Pt(OTf)₂ was selected as the 90° Pt(II) linker for the coordination-driven assembly. The absorption and emission studies of the obtained cage **52** presented the blue/red ratiometric emission changes corresponding to the variation of the oxygen (O₂) or nitrogen (N₂) atmosphere (Figure 12b–d). The encapsulation of cage **52** into an amphiphilic polymer methylpoly(ethyleneglycol)-block-poly(*g*-benzyl-L-glutamate) provided the metallacage-loaded nanoparticles with a loading efficiency of 65%, which could be further applied to detect the hypoxia environment both *in vitro* and *in vivo* (Figure 12e,f). *In vivo* studies indicated that the nanoformulations not only showed ratiometric imaging of the tumor hypoxia condition, but also were capable of effectively suppressing the tumor growth.

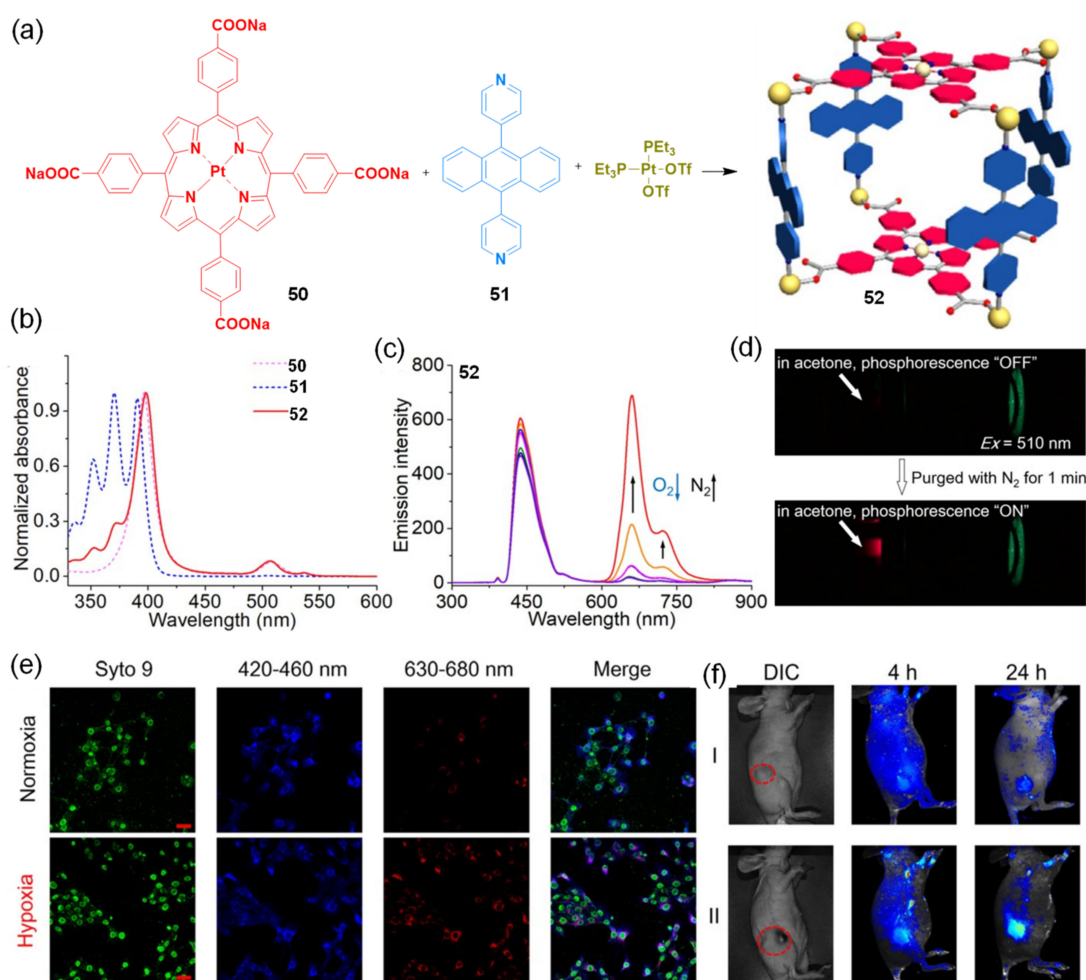


Figure 12. Dual-emissive Pt(II) metallacage and properties. (a) Synthesis of metallacage **52**. (b) Normalized absorption spectra of **50**, **51**, and **52**. (c) Emission spectra of **52** excited at 390 nm under O₂ or N₂ condition. (d) Photos of the emissions of an acetone solution of **52** in a quartz cuvette. (e) Confocal laser scanning microscopy of 4T1 cells stained by Syto 9 and the metallacage loaded nanoparticles. (f) *In vivo* fluorescent images. Reprinted with permission from Ref. [97]. Copyright 2020 John Wiley and Sons.

4. Conclusions and Outlook

Though the assemblies and functions of metallacycles and metallacages have been reviewed on many occasions [3,4,6–8,18], the specific topic on the anthracene-containing met-

allacycles and metallacages has not been surveyed in the literature. This review article summarizes for the first time the anthracene-containing metallacycles and metallacages with diverse shapes and sizes that are constructed by the facile and controllable coordination-driven self-assembly methodology. The modification of the anthracene backbone with different functional and/or directional moieties leads to the formation of corresponding supramolecular architectures with unique photophysical and photochemical behavior and a variety of confined cavities. In line with these properties, many of these structures have been explored in various applications such as host–guest chemistry, stimulus response, molecular sensing, light harvesting energy transfer and biomedical science. These results are expected to give insightful information to stimulate the design and preparation of functional coordination supramolecular assemblies.

Regarding the future development of the structural diversity and potential applications in this field, some aspects may be considered. On the one hand, the current functionalization of anthracene mainly focuses on the monomer-based derivatives. The construction of supramolecular scaffolds with ligands containing an anthracene dimer, or even a trimeric structure, remains under-explored, though a few of examples have proven that the anthracene dimer-based supramolecular scaffolds can exhibit sensitive stimulus-responsive fluorescence properties due to their expanded large aromatic conjugation and inter/intra molecular stackings. On the other hand, upgrading the current platforms toward practical applications is highly desired. For instance, in the case of the singlet oxygen-capture and -release systems, it is still challenging to achieve these functions under physiological condition, which is critical to the oxygen-independent photodynamic therapy of hypoxic tumors.

Author Contributions: Conceptualization and writing, J.-H.T. and Y.-W.Z.; supervision, Y.-W.Z.; funding acquisition, Y.-W.Z. All authors have read and agreed to the published version of the manuscript.

Funding: National Natural Science Foundation of China; Funding numbers: 21872154 and 21925112. Beijing Natural Science Foundation; Funding number: 2191003.

Institutional Review Board Statement: Not applicable.

Informed Consent Statement: Not applicable.

Data Availability Statement: Data sharing not applicable.

Conflicts of Interest: The authors declare no conflict of interest. J.-H.T. is currently a postdoctoral fellow at Northwestern University with no competing interests.

References

1. Gianneschi, N.C.; Masar, M.S.; Mirkin, C.A. Development of a Coordination Chemistry-Based Approach for Functional Supramolecular Structures. *Acc. Chem. Res.* **2005**, *38*, 825–837. [[CrossRef](#)] [[PubMed](#)]
2. Atwood, J.L.; Barbour, L.J.; Hardie, M.J.; Raston, C.L. Metal sulfonatocalix[4,5]arene complexes: Bi-layers, capsules, spheres, tubular arrays and beyond. *Coord. Chem. Rev.* **2001**, *222*, 3–32. [[CrossRef](#)]
3. Cook, T.R.; Zheng, Y.-R.; Stang, P.J. Metal–organic frameworks and self-assembled supramolecular coordination complexes: Comparing and contrasting the design, synthesis, and functionality of metal–organic materials. *Chem. Rev.* **2013**, *113*, 734–777. [[CrossRef](#)] [[PubMed](#)]
4. Wang, W.; Wang, Y.-X.; Yang, H.-B. Supramolecular transformations within discrete coordination-driven supramolecular architectures. *Chem. Soc. Rev.* **2016**, *45*, 2656–2693. [[CrossRef](#)]
5. Zhu, H.; Li, Q.; Khalil-Cruz, L.E.; Khashab, N.M.; Yu, G.; Huang, F. Pillararene-based supramolecular systems for theranostics and bioapplications. *Sci. China Chem.* **2021**, *64*, 688–700. [[CrossRef](#)]
6. Tuo, W.; Xu, Y.; Fan, Y.; Li, J.; Qiu, M.; Xiong, X.; Li, X.; Sun, Y. Biomedical applications of Pt (II) metallacycle/metallacage-based agents: From mono-chemotherapy to versatile imaging contrasts and theranostic platforms. *Coord. Chem. Rev.* **2021**, *443*, 214017. [[CrossRef](#)]
7. Cook, T.R.; Stang, P.J. Recent developments in the preparation and chemistry of metallacycles and metallacages via coordination. *Chem. Rev.* **2015**, *115*, 7001–7045. [[CrossRef](#)]
8. Wu, G.-Y.; Chen, L.-J.; Xu, L.; Zhao, X.-L.; Yang, H.-B. Construction of supramolecular hexagonal metallacycles via coordination-driven self-assembly: Structure, properties and application. *Coord. Chem. Rev.* **2018**, *369*, 39–75. [[CrossRef](#)]
9. Ballester, P.; Fujita, M.; Rebek, J. Molecular containers. *Chem. Soc. Rev.* **2015**, *44*, 392–393. [[CrossRef](#)]

10. Samanta, S.K.; Isaacs, L. Biomedical applications of metal organic polygons and polyhedra (MOPs). *Coord. Chem. Rev.* **2020**, *410*, 213181. [[CrossRef](#)]
11. Li, Y.; Yu, J.-G.; Ma, L.-L.; Li, M.; An, Y.-Y.; Han, Y.-F. Strategies for the construction of supramolecular assemblies from poly-NHC ligand precursors. *Sci. China Chem.* **2021**, *64*, 701–718. [[CrossRef](#)]
12. Zarra, S.; Wood, D.M.; Roberts, D.A.; Nitschke, J.R. Molecular containers in complex chemical systems. *Chem. Soc. Rev.* **2015**, *44*, 419–432. [[CrossRef](#)]
13. Dey, N.; Haynes, C.J. Supramolecular Coordination Complexes as Optical Biosensors. *ChemPlusChem* **2021**, *86*, 418–433. [[CrossRef](#)]
14. Yoshizawa, M.; Klosterman, J.K. Molecular architectures of multi-anthracene assemblies. *Chem. Soc. Rev.* **2014**, *43*, 1885–1898. [[CrossRef](#)]
15. Yoshizawa, M.; Catti, L. Bent Anthracene Dimers as Versatile Building Blocks for Supramolecular Capsules. *Acc. Chem. Res.* **2019**, *52*, 2392–2404. [[CrossRef](#)]
16. Wright, W.H. Ultraviolet Properties of Crystalline Anthracene. *Chem. Rev.* **1967**, *67*, 581–597. [[CrossRef](#)]
17. Huang, J.; Su, J.-H.; Tian, H. The development of anthracene derivatives for organic light-emitting diodes. *J. Mater. Chem.* **2012**, *22*, 10977–10989. [[CrossRef](#)]
18. Sun, Y.; Stang, P.J. Metallacycles, metallacages, and their aggregate/optical behavior. *Aggregate* **2021**, *2*, e94. [[CrossRef](#)]
19. Tidmarsh, I.S.; Faust, T.B.; Adams, H.; Harding, L.P.; Russo, L.; Clegg, W.; Ward, M.D. Octanuclear cubic coordination cages. *J. Am. Chem. Soc.* **2008**, *130*, 15167–15175. [[CrossRef](#)]
20. Vasylevskiy, S.I.; Regeta, K.; Ruggi, A.; Petoud, S.; Piguët, C.; Fromm, K.M. cis- and trans-9,10-di(1H-imidazol-1-yl)-anthracene based coordination polymers of ZnII and CdII: Synthesis, crystal structures and luminescence properties. *Dalton Trans.* **2018**, *47*, 596–607. [[CrossRef](#)]
21. Sinha, N.; Hahn, F.E. Metallosupramolecular Architectures Obtained from Poly-N-heterocyclic Carbene Ligands. *Acc. Chem. Res.* **2017**, *50*, 2167–2184. [[CrossRef](#)]
22. Kuehl, C.J.; Mayne, C.L.; Arif, A.M.; Stang, P.J. Coordination-Driven Assembly of Molecular Rectangles via an Organometallic “Clip”. *Org. Lett.* **2000**, *2*, 3727–3729. [[CrossRef](#)]
23. Brocker, E.R.; Anderson, S.E.; Northrop, B.H.; Stang, P.J.; Bowers, M.T. Structures of Metallosupramolecular Coordination Assemblies Can Be Obtained by Ion Mobility Spectrometry–Mass Spectrometry. *J. Am. Chem. Soc.* **2010**, *132*, 13486–13494. [[CrossRef](#)]
24. Ronson, T.K.; Pilgrim, B.S.; Nitschke, J.R. Pathway-Dependent Post-assembly Modification of an Anthracene-Edged MII4L6 Tetrahedron. *J. Am. Chem. Soc.* **2016**, *138*, 10417–10420. [[CrossRef](#)]
25. Liu, W.; Stoddart, J.F. Emergent behavior in nanoconfined molecular containers. *Chem* **2021**, *7*, 919–947. [[CrossRef](#)]
26. Karslyan, E.E.; Borissova, A.O.; Perekalin, D.S. Ligand Design for Site-Selective Metal Coordination: Synthesis of Transition-Metal Complexes with η⁶-Coordination of the Central Ring of Anthracene. *Angew. Chem. Int. Ed.* **2017**, *56*, 5584–5587. [[CrossRef](#)]
27. Luo, D.; Wu, L.-X.; Zhang, Y.; Huang, Y.-L.; Chen, X.-L.; Zhou, X.-P.; Li, D. Self-assembly of a photoluminescent metal-organic cage and its spontaneous aggregation in dilute solutions enabling time-dependent emission enhancement. *Sci. China Chem.* **2022**, *65*, 1105–1111. [[CrossRef](#)]
28. Lehn, J.M. Perspectives in supramolecular chemistry—from molecular recognition towards molecular information processing and self-organization. *Angew. Chem. Int. Ed.* **1990**, *29*, 1304–1319. [[CrossRef](#)]
29. Li, C.; Jia, P.-P.; Xu, Y.-L.; Ding, F.; Yang, W.-C.; Sun, Y.; Li, X.-P.; Yin, G.-Q.; Xu, L.; Yang, G.-F. Photoacoustic imaging-guided chemo-photothermal combinational therapy based on emissive Pt (II) metallacycle-loaded biomimic melanin dots. *Sci. China Chem.* **2021**, *64*, 134–142. [[CrossRef](#)]
30. Kishi, N.; Li, Z.; Yoza, K.; Akita, M.; Yoshizawa, M. An M2L4 molecular capsule with an anthracene shell: Encapsulation of large guests up to 1 nm. *J. Am. Chem. Soc.* **2011**, *133*, 11438–11441. [[CrossRef](#)]
31. Zhou, Y.; Zhang, H.-Y.; Zhang, Z.-Y.; Liu, Y. Tunable Luminescent Lanthanide Supramolecular Assembly Based on Photoreaction of Anthracene. *J. Am. Chem. Soc.* **2017**, *139*, 7168–7171. [[CrossRef](#)] [[PubMed](#)]
32. McConnell, A.J.; Wood, C.S.; Neelakandan, P.P.; Nitschke, J.R. Stimuli-Responsive Metal–Ligand Assemblies. *Chem. Rev.* **2015**, *115*, 7729–7793. [[CrossRef](#)] [[PubMed](#)]
33. Shanmugaraju, S.; Mukherjee, P.S. Self-Assembled Discrete Molecules for Sensing Nitroaromatics. *Chem. Eur. J.* **2015**, *21*, 6656–6666. [[CrossRef](#)] [[PubMed](#)]
34. Ghosh, S.; Chakrabarty, R.; Mukherjee, P.S. Design, Synthesis, and Characterizations of a Series of Pt₄ Macrocycles and Fluorescent Sensing of Fe³⁺/Cu²⁺/Ni²⁺ Through Metal Coordination. *Inorg. Chem.* **2009**, *48*, 549–556. [[CrossRef](#)]
35. Mukherjee, P.S.; Min, K.S.; Arif, A.M.; Stang, P.J. Synthesis and Crystal Structure of Two New Discrete, Neutral Complexes of Manganese and Zinc Using a Rigid Organic Clip. *Inorg. Chem.* **2004**, *43*, 6345–6350. [[CrossRef](#)]
36. Bar, A.K.; Shanmugaraju, S.; Chi, K.-W.; Mukherjee, P.S. Self-assembly of neutral and cationic PdII organometallic molecular rectangles: Synthesis, characterization and nitroaromatic sensing. *Dalton Trans.* **2011**, *40*, 2257–2267. [[CrossRef](#)]
37. Ghosh, S.; Mukherjee, P.S. Self-assembly of metal–organic hybrid nanoscopic rectangles. *Dalton Trans.* **2007**, *36*, 2542–2546. [[CrossRef](#)]
38. Shanmugaraju, S.; Joshi, S.A.; Mukherjee, P.S. Self-Assembly of Metallamacrocycles Using a Dinuclear Organometallic Acceptor: Synthesis, Characterization, and Sensing Study. *Inorg. Chem.* **2011**, *50*, 11736–11745. [[CrossRef](#)]

39. Shanmugaraju, S.; Bar, A.K.; Jadhav, H.; Moon, D.; Mukherjee, P.S. Coordination self-assembly of tetranuclear Pt(II) macrocycles with an organometallic backbone for sensing of acyclic dicarboxylic acids. *Dalton Trans.* **2013**, *42*, 2998–3008. [[CrossRef](#)]
40. Shanmugaraju, S.; Bar, A.K.; Joshi, S.A.; Patil, Y.P.; Mukherjee, P.S. Constructions of 2D-Metallamacrocycles Using Half-Sandwich Ru(II) Precursors: Synthesis, Molecular Structures, and Self-Selection for a Single Linkage Isomer. *Organometallics* **2011**, *30*, 1951–1960. [[CrossRef](#)]
41. Kryschenko, Y.K.; Seidel, S.R.; Muddiman, D.C.; Nepomuceno, A.I.; Stang, P.J. Coordination-Driven Self-Assembly of Supramolecular Cages: Heteroatom-Containing and Complementary Trigonal Prisms. *J. Am. Chem. Soc.* **2003**, *125*, 9647–9652. [[CrossRef](#)]
42. Ghosh, S.; Gole, B.; Bar, A.K.; Mukherjee, P.S. Self-Assembly of Molecular Prisms via Pt(III) Organometallic Acceptors and a Pt(II) Organometallic Clip. *Organometallics* **2009**, *28*, 4288–4296. [[CrossRef](#)]
43. Shan, W.L.; Lin, Y.J.; Hahn, F.E.; Jin, G.X. Highly Selective Synthesis of Iridium (III) Metalla [2] catenanes through Component Pre-Orientation by $\pi \cdots \pi$ Stacking. *Angew. Chem. Int. Ed.* **2019**, *58*, 5882–5886. [[CrossRef](#)]
44. Hahn, F.E.; Jahnke, M.C. Heterocyclic Carbenes: Synthesis and Coordination Chemistry. *Angew. Chem. Int. Ed.* **2008**, *47*, 3122–3172. [[CrossRef](#)]
45. Credendino, R.; Falivene, L.; Cavallo, L. π -Face Donation from the Aromatic N-Substituent of N-Heterocyclic Carbene Ligands to Metal and Its Role in Catalysis. *J. Am. Chem. Soc.* **2012**, *134*, 8127–8135. [[CrossRef](#)]
46. Velazquez, H.D.; Verpoort, F. N-heterocyclic carbene transition metal complexes for catalysis in aqueous media. *Chem. Soc. Rev.* **2012**, *41*, 7032–7060. [[CrossRef](#)]
47. Visbal, R.; Gimeno, M.C. N-heterocyclic carbene metal complexes: Photoluminescence and applications. *Chem. Soc. Rev.* **2014**, *43*, 3551–3574. [[CrossRef](#)]
48. Mercks, L.; Albrecht, M. Beyond catalysis: N-heterocyclic carbene complexes as components for medicinal, luminescent, and functional materials applications. *Chem. Soc. Rev.* **2010**, *39*, 1903–1912. [[CrossRef](#)]
49. Lin, C.-X.; Kong, X.-F.; Li, Q.-S.; Zhang, Z.-Z.; Yuan, Y.-F.; Xu, F.-B. Dinuclear Ag(I) metallamacrocycles of bis-N-heterocyclic carbenes bridged by calixarene fragments: Synthesis, structure and chemosensing behavior. *CrystEngComm* **2013**, *15*, 6948–6962. [[CrossRef](#)]
50. Megyes, T.; Jude, H.; Grósz, T.; Bakó, I.; Radnai, T.; Tárkányi, G.; Pálincás, G.; Stang, P.J. X-ray diffraction and DOSY NMR characterization of self-assembled supramolecular metalocyclic species in solution. *J. Am. Chem. Soc.* **2005**, *127*, 10731–10738. [[CrossRef](#)]
51. Goldberg, J.M.; Guard, L.M.; Wong, G.W.; Brayton, D.F.; Kaminsky, W.; Goldberg, K.I.; Heinekey, D.M. Preparation and Reactivity of Bimetallic (pincer)Ir Complexes. *Organometallics* **2020**, *39*, 3323–3334. [[CrossRef](#)]
52. Resendiz, M.J.; Noveron, J.C.; Disteldorf, H.; Fischer, S.; Stang, P.J. A self-assembled supramolecular optical sensor for Ni (II), Cd (II), and Cr (III). *Org. Lett.* **2004**, *6*, 651–653. [[CrossRef](#)]
53. Gong, J.-R.; Wan, L.-J.; Yuan, Q.-H.; Bai, C.-L.; Jude, H.; Stang, P.J. Mesoscopic self-organization of a self-assembled supramolecular rectangle on highly oriented pyrolytic graphite and Au (111) surfaces. *Proc. Natl. Acad. Sci. USA* **2005**, *10*, 971–974. [[CrossRef](#)]
54. Kuehl, C.J.; Kryschenko, Y.K.; Radhakrishnan, U.; Seidel, S.R.; Huang, S.D.; Stang, P.J. Self-assembly of nanoscopic coordination cages of D_{3h} symmetry. *Proc. Natl. Acad. Sci. USA* **2002**, *99*, 4932–4936. [[CrossRef](#)]
55. Zheng, Y.-R.; Yang, H.-B.; Northrop, B.H.; Ghosh, K.; Stang, P.J. Size selective self-sorting in coordination-driven self-assembly of finite ensembles. *Inorg. Chem.* **2008**, *47*, 4706–4711. [[CrossRef](#)]
56. Yang, H.-B.; Ghosh, K.; Northrop, B.H.; Stang, P.J. Self-recognition in the coordination-driven self-assembly of three-dimensional M₃L₂ polyhedra. *Org. Lett.* **2007**, *9*, 1561–1564. [[CrossRef](#)]
57. Das, N.; Mukherjee, P.S.; Arif, A.M.; Stang, P.J. Facile self-assembly of predesigned neutral 2D Pt-macrocycles via a new class of rigid oxygen donor linkers. *J. Am. Chem. Soc.* **2003**, *125*, 13950–13951. [[CrossRef](#)]
58. Das, N.; Arif, A.M.; Stang, P.J.; Sieger, M.; Sarkar, B.; Kaim, W.; Fiedler, J. Self-assembly of heterobimetallic neutral macrocycles incorporating ferrocene spacer groups: Spectroelectrochemical analysis of the double two-electron oxidation of a molecular rectangle. *Inorg. Chem.* **2005**, *44*, 5798–5804. [[CrossRef](#)]
59. Das, N.; Stang, P.J.; Arif, A.M.; Campana, C.F. Synthesis and structural characterization of carborane-containing neutral, self-assembled Pt-metallacycles. *J. Org. Chem.* **2005**, *70*, 10440–10446. [[CrossRef](#)]
60. Huang, F.; Yang, H.-B.; Das, N.; Maran, U.; Arif, A.M.; Gibson, H.W.; Stang, P.J. Incorporating a flexible crown ether into neutral discrete self-assemblies driven by metal coordination. *J. Org. Chem.* **2006**, *71*, 6623–6625. [[CrossRef](#)]
61. Das, N.; Ghosh, A.; Singh, O.M.; Stang, P.J. Facile synthesis of enantiopure chiral molecular rectangles exhibiting induced circular dichroism. *Org. Lett.* **2006**, *8*, 1701–1704. [[CrossRef](#)] [[PubMed](#)]
62. Bar, A.K.; Gole, B.; Ghosh, S.; Mukherjee, P.S. Self-assembly of a Pd(II) neutral molecular rectangle via a new organometallic Pd(II) molecular clip and oxygen donor linker. *Dalton Trans.* **2009**, *38*, 6701–6704. [[CrossRef](#)] [[PubMed](#)]
63. Debata, N.B.; Tripathy, D.; Chand, D.K. Self-assembled coordination complexes from various palladium(II) components and bidentate or polydentate ligands. *Coord. Chem. Rev.* **2012**, *256*, 1831–1945. [[CrossRef](#)]
64. Sommer, S.K.; Henle, E.A.; Zakharov, L.N.; Pluth, M.D. Selection for a Single Self-Assembled Macrocycle from a Hybrid Metal-Ligand Hydrogen-Bonded (MLHB) Ligand Subunit. *Inorg. Chem.* **2015**, *54*, 6910–6916. [[CrossRef](#)] [[PubMed](#)]
65. Yeung, M.C.-L.; Yam, V.W.-W. Luminescent cation sensors: From host-guest chemistry, supramolecular chemistry to reaction-based mechanisms. *Chem. Soc. Rev.* **2015**, *44*, 4192–4202. [[CrossRef](#)] [[PubMed](#)]

66. Pluth, M.D.; Raymond, K.N. Reversible guest exchange mechanisms in supramolecular host–guest assemblies. *Chem. Soc. Rev.* **2007**, *36*, 161–171. [[CrossRef](#)]
67. Yang, X.; Yuan, D.; Hou, J.; Sedgwick, A.C.; Xu, S.; James, T.D.; Wang, L. Organic/inorganic supramolecular nano-systems based on host/guest interactions. *Coord. Chem. Rev.* **2021**, *428*, 213609. [[CrossRef](#)]
68. Wei, P.; Yan, X.; Huang, F. Supramolecular polymers constructed by orthogonal self-assembly based on host–guest and metal–ligand interactions. *Chem. Soc. Rev.* **2015**, *44*, 815–832. [[CrossRef](#)]
69. Qu, D.-H.; Wang, Q.-C.; Zhang, Q.-W.; Ma, X.; Tian, H. Photoresponsive host–guest functional systems. *Chem. Rev.* **2015**, *115*, 7543–7588. [[CrossRef](#)]
70. Lee, H.; Elumalai, P.; Singh, N.; Kim, H.; Lee, S.U.; Chi, K.-W. Selective synthesis of ruthenium (II) metalla [2] catenane via solvent and guest-dependent self-assembly. *J. Am. Chem. Soc.* **2015**, *137*, 4674–4677. [[CrossRef](#)]
71. Yamashina, M.; Sartin, M.M.; Sei, Y.; Akita, M.; Takeuchi, S.; Tahara, T.; Yoshizawa, M. Preparation of highly fluorescent host–guest complexes with tunable color upon encapsulation. *J. Am. Chem. Soc.* **2015**, *137*, 9266–9269. [[CrossRef](#)]
72. Kuwabara, J.; Stern, C.L.; Mirkin, C.A. A coordination chemistry approach to a multieffector enzyme mimic. *J. Am. Chem. Soc.* **2007**, *129*, 10074–10075. [[CrossRef](#)]
73. Wang, Y.; Zhang, Y.-M.; Zhang, S.X.-A. Stimuli-Induced Reversible Proton Transfer for Stimuli-Responsive Materials and Devices. *Acc. Chem. Res.* **2021**, *54*, 2216–2226. [[CrossRef](#)]
74. Møllerup, S.K.; Wang, S. Boron-based stimuli responsive materials. *Chem. Soc. Rev.* **2019**, *48*, 3537–3549. [[CrossRef](#)]
75. Wang, X.; Wang, X.; Jin, S.; Muhammad, N.; Guo, Z. Stimuli-responsive therapeutic metallodrugs. *Chem. Rev.* **2018**, *119*, 1138–1192. [[CrossRef](#)]
76. Tang, J.-H.; Sun, Y.; Gong, Z.-L.; Li, Z.-Y.; Zhou, Z.; Wang, H.; Li, X.; Saha, M.L.; Zhong, Y.-W.; Stang, P.J. Temperature-Responsive Fluorescent Organoplatinum(II) Metallacycles. *J. Am. Chem. Soc.* **2018**, *140*, 7723–7729. [[CrossRef](#)]
77. Chen, Z.; Tang, J.-H.; Chen, W.; Xu, Y.; Wang, H.; Zhang, Z.; Sepehrpour, H.; Cheng, G.-J.; Li, X.; Wang, P. Temperature- and mechanical-force-responsive self-assembled rhomboidal metallacycle. *Organometallics* **2019**, *38*, 4244–4249. [[CrossRef](#)]
78. Yu, H.; Shi, J.; Li, M.; Pan, G.; Tong, H.; Xu, B.; Wang, M.; Tian, W. Discrete Platinum (II) Metallacycles with Inner- and Outer-Modified 9, 10-Distyrylanthracene: Design, Self-Assembly, and Luminescence Properties. *Inorg. Chem.* **2022**, *61*, 7231–7237. [[CrossRef](#)]
79. Twilton, J.; Le, C.; Zhang, P.; Shaw, M.H.; Evans, R.W.; MacMillan, D.W.C. The merger of transition metal and photocatalysis. *Nat. Rev. Chem.* **2017**, *1*, 0052. [[CrossRef](#)]
80. Bisoyi, H.K.; Li, Q. Light-Driven Liquid Crystalline Materials: From Photo-Induced Phase Transitions and Property Modulations to Applications. *Chem. Rev.* **2016**, *116*, 15089–15166. [[CrossRef](#)]
81. Becker, H.D. Unimolecular photochemistry of anthracenes. *Chem. Rev.* **1993**, *93*, 145–172. [[CrossRef](#)]
82. Bai, S.; Wang, L.-F.; Wu, Z.-W.; Feng, T.; Han, Y.-F. Supramolecular-controlled regioselective photochemical [4 + 4] cycloaddition within Cp*Rh-based metallarectangles. *Dalton Trans.* **2022**, *51*, 8743–8748. [[CrossRef](#)]
83. Bai, S.; Ma, L.-L.; Yang, T.; Wang, F.; Wang, L.-F.; Hahn, F.E.; Wang, Y.-Y.; Han, Y.-F. Supramolecular-induced regiocontrol over the photochemical [4 + 4] cycloaddition of NHC- or azole-substituted anthracenes. *Chem. Sci.* **2021**, *12*, 2165–2171. [[CrossRef](#)]
84. Omoto, K.; Tashiro, S.; Shionoya, M. Phase-Dependent Reactivity and Host–Guest Behaviors of a Metallo-Macrocycle in Liquid and Solid-State Photosensitized Oxygenation Reactions. *J. Am. Chem. Soc.* **2021**, *143*, 5406–5412. [[CrossRef](#)]
85. He, Y.-Q.; Fudickar, W.; Tang, J.-H.; Wang, H.; Li, X.; Han, J.; Wang, Z.; Liu, M.; Zhong, Y.-W.; Linker, T. Capture and release of singlet oxygen in coordination-driven self-assembled organoplatinum (II) metallacycles. *J. Am. Chem. Soc.* **2020**, *142*, 2601–2608. [[CrossRef](#)] [[PubMed](#)]
86. Guo, C.; Sedgwick, A.C.; Hirao, T.; Sessler, J.L. Supramolecular fluorescent sensors: An historical overview and update. *Coord. Chem. Rev.* **2021**, *427*, 213560. [[CrossRef](#)] [[PubMed](#)]
87. Mako, T.L.; Racicot, J.M.; Levine, M. Supramolecular Luminescent Sensors. *Chem. Rev.* **2019**, *119*, 322–477. [[CrossRef](#)] [[PubMed](#)]
88. You, L.; Zha, D.; Anslyn, E.V. Recent Advances in Supramolecular Analytical Chemistry Using Optical Sensing. *Chem. Rev.* **2015**, *115*, 7840–7892. [[CrossRef](#)]
89. Zhang, M.; Saha, M.L.; Wang, M.; Zhou, Z.; Song, B.; Lu, C.; Yan, X.; Li, X.; Huang, F.; Yin, S.; et al. Multicomponent Platinum(II) Cages with Tunable Emission and Amino Acid Sensing. *J. Am. Chem. Soc.* **2017**, *139*, 5067–5074. [[CrossRef](#)] [[PubMed](#)]
90. Saha, M.L.; Yan, X.; Stang, P.J. Photophysical properties of organoplatinum(II) compounds and derived self-assembled metallacycles and metallacages: Fluorescence and its applications. *Acc. Chem. Res.* **2016**, *49*, 2527–2539. [[CrossRef](#)]
91. Li, Z.; Yan, X.; Huang, F.; Sepehrpour, H.; Stang, P.J. Near-infrared emissive discrete platinum (II) metallacycles: Synthesis and application in ammonia detection. *Org. Lett.* **2017**, *19*, 5728–5731. [[CrossRef](#)]
92. Yamashina, M.; Akita, M.; Hasegawa, T.; Hayashi, S.; Yoshizawa, M. A polyaromatic nanocapsule as a sucrose receptor in water. *Sci. Adv.* **2017**, *3*, e1701126. [[CrossRef](#)]
93. Ajayaghosh, A.; Praveen, V.K.; Vijayakumar, C. Organogels as scaffolds for excitation energy transfer and light harvesting. *Chem. Soc. Rev.* **2008**, *37*, 109–122. [[CrossRef](#)]
94. Hu, F.; Xu, S.; Liu, B. Photosensitizers with aggregation-induced emission: Materials and biomedical applications. *Adv. Mater.* **2018**, *30*, 1801350. [[CrossRef](#)]

95. Jia, P.-P.; Xu, L.; Hu, Y.-X.; Li, W.-J.; Wang, X.-Q.; Ling, Q.-H.; Shi, X.; Yin, G.-Q.; Li, X.; Sun, H. Orthogonal self-assembly of a two-step fluorescence-resonance energy transfer system with improved photosensitization efficiency and photooxidation activity. *J. Am. Chem. Soc.* **2020**, *143*, 399–408. [[CrossRef](#)]
96. Li, Y.; Rajasree, S.S.; Lee, G.Y.; Yu, J.; Tang, J.-H.; Ni, R.; Li, G.; Houk, K.N.; Deria, P.; Stang, P.J. Anthracene–Triphenylamine-Based Platinum (II) Metallacages as Synthetic Light-Harvesting Assembly. *J. Am. Chem. Soc.* **2021**, *143*, 2908–2919. [[CrossRef](#)]
97. Zhu, H.; Li, Q.; Shi, B.; Ge, F.; Liu, Y.; Mao, Z.; Zhu, H.; Wang, S.; Yu, G.; Huang, F. Dual-emissive platinum (II) metallacage with a sensitive oxygen response for imaging of hypoxia and imaging-guided chemotherapy. *Angew. Chem. Int. Ed.* **2020**, *59*, 20208–20214. [[CrossRef](#)]